

ACTIVE FREQUENCY DRIFT ISLANDING DETECTION ALGORITHM FOR SINGLE-PHASE PHOTOVOLTAIC GRID-CONNECTED INVERTER

A. Guangping Lu*

B. Lanhong Zhang

D. Yunlong Zhou

School of Electrical Engineering

Yancheng Institute of Technology

Jiangsu

China

luguangp@hotmail.com

C. Yingchu Bu

Infrastructure Construction Department

Yancheng Institute of Technology

Jiangsu

China

Abstract. As the photovoltaic generation industry rises, the requirements for the reliability of photovoltaic power generation have become higher. The traditional active frequency drift islanding detection algorithm has advantages of simple operation, easy implementation, high speed and high detection rate of island; however, the large impact of the algorithm on the detection performance can bring harmonic pollution to power grid and even induce voltage flicker and instability of the network system. When multiple photovoltaic systems work in the form of grid connection, frequency drift appears and the effects cancel each other out, leading to the appearance of non-detection zones.

This study simulated a positive feedback islanding detection method using SIMULINK and proposed a novel active positive feedback active frequency drift detection method that could realize frequency drift by increasing disturbance with piecewise function based on the drawbacks of the active frequency drift islanding detection algorithm. Finally, the advantages of the system in resisting islanding were verified through computer simulation.

Keywords: inverter; enhancement; active frequency drift detection method; computer simulation software; islanding detection.

1. Introduction

Principle component analysis can process a problem of high-latitude space by transforming it into a problem of low-latitude space [1, 2], thus to make the problem simpler and more visualized. Moreover, in the process of principal component analysis, each principal component will generate its weight auto-

*. Corresponding author

matically [3], which resists the influence of human factors in evaluation process and makes evaluation results more objective. Principal component analysis can be divided into principal component analysis for population and principal component analysis for samples [4]. In the analysis of practical problems, population correlation coefficient matrix and covariance matrix are generally unknown; therefore, correlation coefficient matrix and sample covariance matrix need to be calculated for the evaluation or hypothesis testing of samples [5]. When practical problems are analyzed using principal component analysis, principal component which can cover population information is selected through changing variable values and moreover further analysis is made on this basis. But, the premise of principal component selection is to suppose that these principal components can cover population information [6]. Therefore, corresponding hypothesis testing is needed to determine whether the processing of follow-up question is feasible. The size of the non-detection zone (NDZ) is the evaluation criterion for islanding detection. Relevant theoretical analyses and experiments have found that, most of passive islanding detection methods have NDZs [4, 5]. Thus this study proposed a kind of active positive feedback active frequency drift detection method and a new algorithm which could reduce the NDZ, risks of current harmonic distortion and harmonic pollution to network system and accurately and efficiently realize islanding detection functions on the basis of the basic algorithm of active frequency detection.

2. A computer model for islanding detection

SIMULINK was selected as the platform for establishing the islanding detection model. Fig. 1 demonstrates an islanding detection model which is composed of S function module, inverter module, output control module, phase-locked loop (PLL) module, etc. The inputs were the voltage frequency and phase of common points. The signals which were output through the detection algorithm produced four pulses under control to command the output. In accordance with IEEE Std.32000-929/UL1741, the scope of frequency protection is 49.3 HZ 50.5 HZ, and the two seconds after network interruption is the time for islanding detection. The detection method will lose efficacy and a NDZ will appear if it is the time after network interruption is more than two seconds [6].

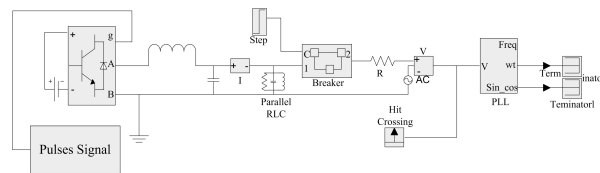


Figure 1: The Islanding Detection Model System

3. A novel positive feedback active frequency drift detection means

The detection method could control the current frequency of the output end of the inverter. The occurrence of islanding could be confirmed if the voltage frequency in the system changed alternately under the interference of disturbance signals. It operated by eliminating the balancing effect of disturbance signals on load under the condition of consistent frequency through adding frequency disturbance signals which were in positive and negative directions and were periodic and continuous into the output of the inverter.

The disturbance signals S_1 and S_2 in two directions were selected and assigned as +5% and -5%. They were added into the network system and turned to be $S_1 + \Delta S_1$ and $S_2 + \Delta S_2$. ΔS_1 and ΔS_2 were the differences between the output frequency of the inverter and the voltage frequency of the original power network. When detection started, S_1 and S_2 disturbed the output frequency of the inverter orderly and alternately, and the values of ΔS_1 and ΔS_2 were compared. When island appeared, the larger one between S_1 and S_2 was regarded as the standard of disturbance signals and added into positive feedback; finally, $S_{k+1} = S_k + \Delta S$ was obtained. ΔS refers to feedback quantity under such control. Due to the high speed of the output end frequency conversion of the inverter, the correlation between the inverter and the power network could be cut off by finding out the island and triggering the protective circuit in a short time [7].

Operation Process

To understand the operation process better, the flow of the positive-feedback active islanding detection is demonstrated in Fig. 2.

Suppose that the power network cut off suddenly, the detailed operation methods taking capacitive load as an example are as follows.

(1) When the disturbance signal $S_2(+5\%)$ disturbed the output frequency of the inverter, its frequency increased. But when the load was capacitive, the voltage became ahead of the current, and the output frequency was smaller than the frequency of the disturbance signals, i.e., $\Delta S_1 < S_1$.

(2) When the disturbance signal $S_2(-5\%)$ disturbed the output frequency of the inverter, the frequency of the inverter decreased. But when the load was capacitive, the voltage became ahead of the current, and the output frequency was larger than the frequency of the disturbance signals, i.e., $\Delta S_2 > S_2$.

(3) As $\Delta S_2 > S_1$, S_2 was selected to interfere the output frequency of the inverter as the criterion of the disturbance signal.

(4) After a series of actions above, the appearance of island could be determined if the specified frequency $f > f_2$, and at that moment, the protective circuit should be triggered immediately.

It could be noted that, the output frequency of the inverter changed obviously when there were island effects whether the load was inductive or capacitive, which eliminated effect offset in single direction. In the system, the disturbance

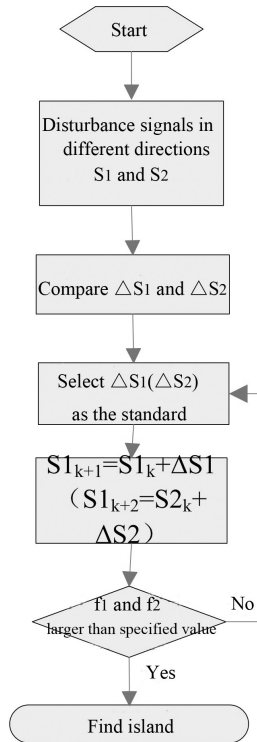


Figure 2: The Flow Diagram of the Islanding Detection Method

signals with large difference values in combination with positive feedback led to the larger variation scope of system frequency, which was beneficial to detect NDZs and accelerate detection; the protective circuit could be triggered to maintain the safety of the whole power network when islanding appeared [8-10].

4. New Algorithms for Detection Methods

The traditional active frequency drift method detects islanding by disturbing assigned frequency with voltage frequency at offset common points at the output end of the inverter, and the quantity of the offset is a fixed value. If power network is cut off, offset will result in unmatched power, inducing the changes in the frequency and amplitude of load voltage. Missing detection may happen if the value of the offset quantity was set too small; load power may be unmatched, thereby increasing the total harmonic distortion if the quantity of offset is too large [11].

To reduce the total harmonic distortion, the current of the inverter was set as segmented periodic current [12].

$$(4.1) \quad i(t) = \begin{cases} I \sin(\omega t), & 0 \leq \omega t \leq \frac{\pi}{2} \\ I \sin(\omega t) - CI, & \frac{\pi}{2} \leq \omega t \leq \pi \\ I \sin(\omega t), & \pi \leq \omega t \leq \frac{3\pi}{2} \\ I \sin(\omega t) + CI, & \frac{3\pi}{2} \leq \omega t \leq 2\pi \end{cases}$$

where I refers to the current amplitude of the inverter and C refers to the frequency distortion factor. The waveform of the new current is demonstrated in Fig. 3. It could be noted from Fig. 3 that, the new current of the inverter had harmonic component. It needed to be processed by Frontier transform. The Frontier coefficient after transformation was:

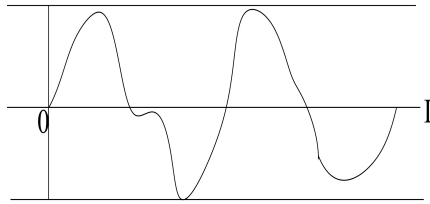


Figure 3: The New Current Waveform of the Inverter

$$(4.2) \quad \begin{aligned} a_n &= \frac{2}{T} \int_{-\frac{T}{2}}^{\frac{T}{2}} I(t) \cos n\omega t dt, \\ b_n &= \frac{2}{T} \int_{-\frac{T}{2}}^{\frac{T}{2}} I(t) \sin n\omega t dt, \\ A_n &= \sqrt{a_n^2 + b_n^2} \text{ and } \Phi_n = \arctan -\frac{b_n}{a_n}. \end{aligned}$$

After specific values were substituted into the above formulas, the Frontier coefficient of the current in the inverter could be obtained.

$$(4.3) \quad a_n = \frac{2CI}{\pi}, b_1 = I(1 - \frac{2C}{\pi}), A_1 = I\sqrt{1 + \frac{8C^2}{\pi^2} - \frac{4C}{\pi}} \text{ and } \Phi_1 = \arctan -\frac{b_1}{a_1}$$

A_1 and Φ_1 are the fundamental wave and phase angle of the new current of the inverter. Consequently, the total harmonic distortion, active power and reactive power of the grid-connected current were obtained

$$(4.4) \quad THD = \sqrt{\frac{C^2(\pi^2 - 8)}{\pi^2 - 4\pi C + 8C^2}}, Q = 2C \text{ and } P = \pi - 2C.$$

Table 1: THD and Q/P of the Two Algorithms

	The value of C	0.075	0.085	0.095
The traditional algorithm	THD and Q/P	5%	5.7%	6.44%
The traditional algorithm	THD and Q/P	5%	5.7%	6.44%
The new algorithm	THD	3.24%	3.90%	4.39%
	Q/P	5%	5.7%	6.44%

When the value of C was different, the aberration rate, active power and reactive power of the grid-connected current of the inverter all changed [13, 14]. Table 1 demonstrates the changes of THD, Q and P of the two algorithms when the value of C was different. It could be noted from Table 1 that, when the Q/P of the two algorithms was the same, the total harmonic distortion of the new algorithm was smaller than that of the traditional algorithm. The algorithm of the traditional detection method added dead time t at the end of two and a half cycles through controlling disturbance signals, while the algorithm of the detection method which was used in this study added dead time t at the end of one cycle to actively control the disturbance of the disturbance signals to the current frequency of the inverter. By doing this, the voltage frequency at the common points would become higher when islanding effect appeared. The property of the load also had impacts on the voltage frequency of the common points [15].

When the load was capacitive, the output end of the inverter selected S_2 as the standard disturbance signal by comparing ΔS_1 and ΔS_2 ; similarly, when the load was inductive, the output end of the inverter selected S_1 as the standard disturbance signal. Fig. 4 shows the comparison of the addition of dead time

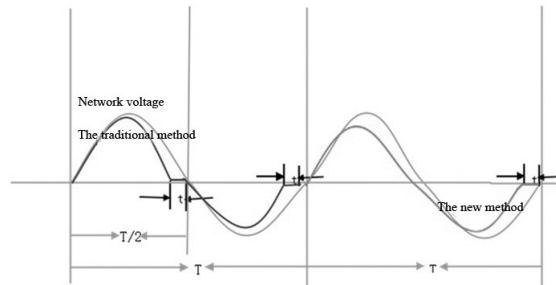


Figure 4: The Control Signals of the Inverter under the Two Algorithms

of two methods given by computer. The size of the NDZ is a vital evaluation criterion for islanding detection. Relevant theoretical analysis and experiments found that, NDZs existed in most of the passive islanding detection methods [16]. In the traditional detection method, the system parameter setting should satisfy $\Phi = \arctan[R(\omega C - \frac{1}{\omega L})] = \frac{\omega t}{2}$; otherwise, overfrequency or underfrequency would happen, leading to NDZs. In the new detection method, the

disturbance signals were controlled in different segments according to the times of frequency changes, and feedback coefficient would not induce large harmonic distortion [17]. As mentioned in the criterion above, the frequency variation times of the common points within two seconds should be less than 10. When the variation times of the common points was more than 10 and the frequency was between 49.3 HZ and 50.5 HZ after power network cut off, the algorithm actively regulated disturbance signals S1 and S2, which could effectively avoid the failure of islanding detection caused by excessively fast frequency changes. With the intensity increase of disturbance signals, NDZs gradually got close to capacitive load interval; however, load is usually inductive in reality. Thus, the NDZ was greatly narrowed. Fig. 5 demonstrates the NDZ of the two algorithms. It could be seen from Fig. 5 that, the NDZ of the new method was smaller than that of the traditional method. The NDZ could be narrowed by correcting parameters, but could not be thoroughly eliminated.

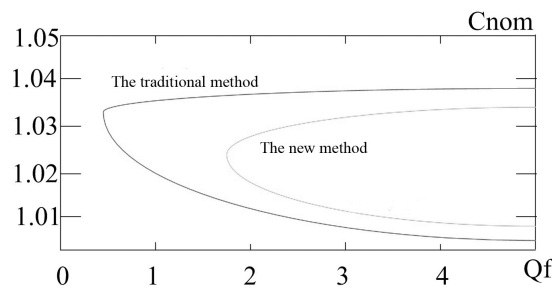


Figure 5: NDZs of the Two Algorithms

5. Experimental simulation of the new detection method

The parameters of the model were set according to the model and islanding detection criteria established above. The NDZ [18] could be the maximum when the output power of the inverter was equal to that of the load, resonant frequency of the Radio Link Control (RLC) parallel circuit reached 50HZ, or load quality factor $Q_f = 2.5$. The parameters at the time when the possibility of islanding detection failure was the highest could be calculated using the given value of Q_f

$$(5.1) \quad Q_f = \frac{2\pi(1/2CR^2I^2)}{\pi RI^2/\omega} = \omega RC = R \frac{1}{\omega L} = \frac{1}{P} \sqrt{Q_L Q_C} = 2.5$$

where R, L, C and I refer to the load resistance, inductance, capacitance and current value respectively, P stands for the load active power, and Q_L and Q_C stand for the inductive reactive power and capacitive reactive power respectively

$$(5.2) \quad P = \frac{U^2}{R}, \quad Q_L = \frac{U^2}{\omega L}, \quad Q_C = U^2 \omega C.$$

The values of the parameters could be obtained by combining the four formulas together

$$(5.3) \quad \begin{cases} R = 15.1\Omega, & L = 21.32mH, & C = 488.6\mu F \\ P = 3KW, & Q_L = 7.535Kvar, & Q_C = 7.535Kvar \end{cases}$$

The above parameters were input into the computer simulation software for the

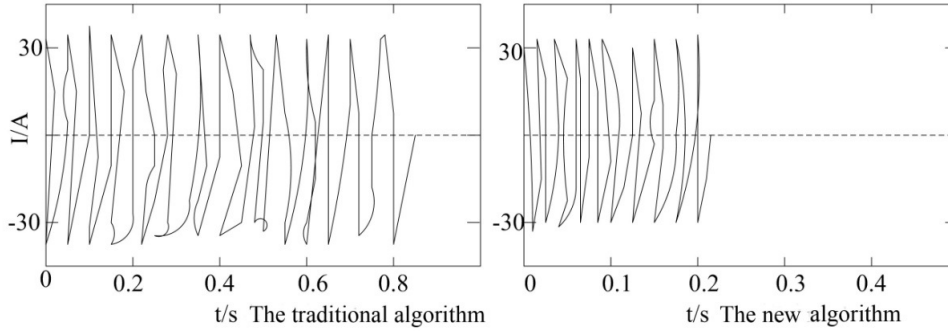


Figure 6: The Waveform of the Output Current of the Inverter under the Two Algorithms

output current simulation of the inverter. Fig. 6 demonstrates the simulation waveform of the output current under the two algorithms.

6. Conclusion

This study proposed a new active frequency drift islanding detection method with feedback on account of the active frequency drift islanding detection. The means could reduce the NDZ in islanding detection and eliminate effect offset in single direction with periodic disturbance signals, which could trigger the protective circuit and maintain the safety of the whole power network when islanding appeared. Moreover, an improved traditional algorithm was introduced; it was verified as qualified for islanding detection through simulation. But the experiment was simulated on the computer platform, lacking practical basis in practical production.

7. Acknowledgements

This work was supported by the D class Six Talent Peak Project in Jiangsu C the development of grid-connected inverter in distributed photovoltaic power generation system (Program No.: 2015-XNY-017).

References

- [1] Q.M. Cheng, Y.F. Wang, Y.M. Cheng, and M.M. Wang, *Overview study on islanding detecting methods for distributed generation grid-connected system*, Power Syst. Protect. Contr., 39 (2011), 147-154.
- [2] A. Yafaoui, B. Wu, S. Kouro, *Improved Active Frequency Drift Antiislanding Detection Method for Grid Connected Photovoltaic Systems*, IEEE Transact. Power Electr., 27 (2012), 2367-2375..
- [3] J.H. Kim, J.G. Kim, Y.H. Ji, Y.C. Jung, C.Y. Won, *An Islanding Detection Method for a Grid-Connected System Based on the Goertzel Algorithm*, IEEE Transact. Power Electr., 26 (4) (2011), 1049-1055.
- [4] H. Pourbabak, A. Kazemi, *Islanding detection method based on a new approach to voltage phase angle of constant power inverters*, IET Gener. Transm. Dis., 10 (2016), 1190-1198.
- [5] Y. Li, M. Hou, H. Feng et al., *Composite islanding detection method based on the active frequency drift and voltage amplitude variation*, Power and Energy Engineering Conference IEEE, (2015)
- [6] Z.W. Liao, H. Liao, Z.Y. Lv, *Active frequency offset detection and blind zone with positive feedback*, Power Electr. Technol., 45 (2011), 27-28.
- [7] P.K. Dash, M. Padhee, T.K. Panigrahi, *A hybrid time-frequency approach based fuzzy logic system for power island detection in grid connected distributed generation*, Int. J. Elec. Power Energ. Syst., 42 (2012), 453-464.
- [8] P. Mahat, Z. Chen, B. Bak-Jensen, *Review of islanding detection methods for distributed generation*, Laser J., 32 (2011), 2743-2748.
- [9] T. Ma, H. Yang, L. Lu, *Performance evaluation of a stand-alone photovoltaic system on an isolated island in Hong Kong*, Appl. Energ., 112 (2013), 663-672.
- [10] W.K.A. Najy, H.H. Zeineldin, A.H.K. Alaboudy, W.L. Woon, *A Bayesian Passive Islanding Detection Method for Inverter-Based Distributed Generation Using ESPRIT*, IEEE Transact. Power Deliv., 26 (2011), 2687-2696.
- [11] X. Lin, X. Dong, Y. Lu, *Application of intelligent algorithm in island detection of distributed generation*, T & D, 2010 IEEE PES, (2010), 1-7.
- [12] R. Bruno, R. Carl, *Border collision bifurcations in a one-dimensional piecewise smooth map for a PWM current-programmed H-bridge inverter*, Int. J. Contr., 75 (2012), 1356-1367.

- [13] J. Farhang, M. Eydi, B. Asaei, B. Farhangi, *Flexible strategy for active and reactive power control in grid connected inverter under unbalanced grid fault*, ICEE, (2015) May 10-14.
- [14] X. Li, R.S. Balog, *PLL-less robust active and reactive power controller for single phase grid-connected inverter with LCL filter*, IEEE, APEC, 2015.
- [15] B. Sun, S.W. Koh, C.A. Yuan, X.J. Fan, G.Q. Zhang, *Accelerated lifetime test for isolated components in linear drivers of high-voltage LED system*, International Conference on Thermal, Mechanical and Multi-Physics Simulation and Experiments in Microelectronics and Microsystems, (2013), 1-5.
- [16] L.B. Yang, Q. Hui, Y. Teng, M. Zong, X. Yu, D.F. Si, X.C. Yu, W. Zhang, *Island Detection System Based on Multi-criteria*, International Conference on Intelligent Transportation, Big Data & Smart City, (2015), 503-506.
- [17] G. Oalumbo, S. Pennisi, *Harmonic distortion in non-linear amplifier with non-linear feedback*, nt. J. Circuit Theor. Appl, 26 (1998), 293-299.
- [18] G. Tsengenes, T. Nathenas, G. Adamidis, *A three-level space vector modulated grid connected inverter with control scheme based on instantaneous power theory*, Simul Model Pract Theor, 25 (2012), 134-147.

Accepted: 9.03.2017